Inorganic Chemistry

ARTICLE

pubs.acs.org/IC

Reevaluation of the Structure and Fundamental Physical Properties of Dawsonites by DFT Studies

Zbigniew Łodziana,*[,†] Georgiana Stoica,[‡] and Javier Pérez-Ramírez[‡]

[†]INP, Polish Academy of Sciences, ul. Radzikowskiego 152, PL-31-342 Kraków, Poland

[‡]Institute for Chemical and Bioengineering, Department of Chemistry and Applied Biosciences, ETH Zurich, HCI E 125, Wolfgang-Pauli-Strasse 10, CH-8093 Zurich, Switzerland

Supporting Information

ABSTRACT: Dawsonite-type compounds, with the general formula $MAlCO_3(OH)_2$, where M = Na^+, K^+, or NH_4^+, recently have become attractive materials because of their potential interest in geochemical CO_2 sequestration, CO_2 capture in power plants, and heterogeneous catalysis. However, the number of studies assessing the properties of these materials is limited. In the present paper, we report a theoretical reevaluation of the structural and essential physicochemical properties of Na-, K-, and NH_4-dawsonites as determined by density functional theory (DFT) investigations. The calculated structure of Na- and K-dawsonites is in good agreement with previous data, while for $NH_4AlCO_3(OH)_2$, the calculations suggest orientation disorder of the ammonium ions in the structure. The normal-mode analysis, electronic and bonding properties, and elastic properties are reported for the three analogue dawsonites. The calculated formation enthalpy is −1714, −1699, and −1655 kJ/mol for K-, Na-, and NH_4-dawsonite, respectively. This study comprises a first step toward a better understanding of the diversity of dawsonite intrinsic properties, which is required to tune their practical applications.

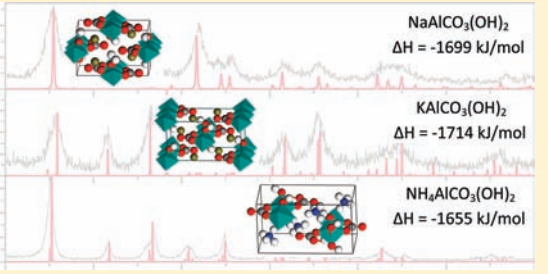

1. INTRODUCTION

Dawsonite ($NaAlCO_3(OH)_2$) was first discovered and collected as "probably new mineral specie" by the Canadian mineralogist John William Dawson in 1862, and named in his honor by Harrington in 1874.[1] Besides $NaAlCO_3(OH)_2$, multiple dawsonite compositions have been synthesized by changing the nature of sodium and/or aluminum cations in the structure.[2−5] Potassium ($KAlCO_3(OH)_2$) and ammonium ($NH_4AlCO_3(OH)_2$) dawsonites are the most studied analogues.

In general, most of the studies related to dawsonites touch upon their geological occurrence as well as their synthesis and characterization. However, recently these compounds are more often reported in relation to CO_2 storage in geological formations,[6−8] as a novel CO_2 capture media in power plants,[9] or with relation to applications in heterogeneous catalysis.[4,5,10−12] Na-dawsonite is claimed to partake in the geochemical fixation of CO_2 by mineral carbonation resulting from the injection of CO_2 into Al-bearing silicate aquifers.[13−15] Generally, dawsonite precipitation occurs at elevated partial pressures of CO_2 and alkaline environments, assured by feldspar dissolution.[7,16−19] Considering the importance of dawsonite in CO_2 sequestration by mineral trapping, we recently studied the stability of synthetic dawsonites ($MAlCO_3(OH)_2$, M = Na^+, K^+, NH_4^+) in a variety of aqueous media (pH 2−14).[20] However, the narrow pH range at which they are stable, i.e., 9−11, poses serious constraints in their potential use for geochemical fixation of CO_2.[20] Nevertheless, spin-offs of the CO_2 storage by natural systems are being considered lately, i.e., CO_2 capture in combustion plants using precursors (alkali-promoted aluminas) leading to dawsonites.[9] Alkali-doped aluminas are efficient adsorbents for CO_2 trapping in the form of carbonates in a relatively stable structure, i.e., dawsonite, via the solid−gas reaction between K_2CO_3-promoted alumina and CO_2 and H_2O (CO_2/steam ratio = 1/1) at 20 bar and 573 K. Carbon dioxide can be released afterward by heat treatment of the resulting dawsonite at 773 K, leading to the regeneration of the alkali-promoted alumina. The authors performed several cycles of adsorption−regeneration at 573 and 773 K, respectively, proving the ability of K-dawsonite ($KAlCO_3(OH)_2$) to be reformed when lowering the temperature. These results extend the area of dawsonite reformation based on the memory effect from the liquid phase[21] to the gas phase, and highlight the potential of dawsonite-derived oxides as efficient adsorbents for industrial CO_2 removal. As the real process of CO_2 capture and storage by dawsonites is rather complex, a hierarchical understanding approach from the bulk material stability to the surface properties is necessary at each reaction step.

The mineral Na-dawsonite was structurally characterized for the first time by Lauro,[22] and the atomically resolved structure, without hydrogen atoms, was reported via X-ray diffraction (XRD) measurements by Frueh and Golightly[23] in 1967. It has a body-centered orthorhombic *Imma* structure with four formula units per unit cell.[24] However, the positions of the hydrogen in

Received: December 7, 2010
Published: February 24, 2011

the $NaAlCO_3(OH)_2$ unit cell were reported 10 years later by Corazza et al.[25] Structural studies were also conducted for K- and NH_4-dawsonite.[26,27] While for K-dawsonite a complete structural picture is available, for the NH_4-analogue the existing structural assignment is based on heavy atoms, without hydrogen. Both compounds, i.e., K- and NH_4-dawsonites, possess base-centered *Cmcm* symmetry,[26,27] thus, they are structurally different from the Na-dawsonite mineral. Moreover, severe differences exist in their response to the environment,[20] while the thermodynamic stability of all three dawsonites seems to be similar.

Detailed knowledge of the crystalline structure is a first and necessary step toward understanding of the physicochemistry of these compounds in the range of low to ultrahigh pressures for geological rocks, low to high temperatures, and aggressive environments for industrial CO_2 capture processes. Insight into the location of the hydrogen atoms in the structure is especially important for this type of compounds because its hydrogen-related vibrations often serve as a spectroscopic fingerprint of a given structure,[28] and the nature and strength of bonds established between hydrogen and the metals or functional groups directly affects the stability of dawsonite.[20,29]

The above-mentioned facts indicate that the properties of Na-dawsonite and the K- and NH_4-analogues must be understood in order to practically develop their promising applications. Present knowledge of these properties is limited, however. Description or design of novel functional materials by means of advanced quantum methods is becoming a state-of-the-art methodology.[30,31] Therefore, solid investigation of the structural, vibrational, or electronic properties is a first step toward design of modified compounds.

The present paper reports the first theoretical study of Na-, K-, and NH_4-dawsonite structural properties by means of density functional theory (DFT) calculations. Our results confirm on a theoretical basis the *Imma* and *Cmcm* structures for Na- and K-dawsonites, while for NH_4-dawsonite, the static configuration in *Cmcm* symmetry appears to be unstable with respect to the rotations of NH_4^+ groups in the crystal lattice. We propose the structure with *Pnma* symmetry, in which it is dynamically stable. The barriers for NH_4 rotations are on the order of 0.3 eV, suggesting possible disorder of the ammonium groups at elevated temperatures. These structures are validated by comparison of the X-ray diffraction patterns with experimental measurements of the synthesized samples. We show that the electronic structure of the three dawsonites and interatomic bonding are similar. Additionally, we report herein their vibrational properties with symmetry assigned normal-mode analysis, their elastic properties, and the formation enthalpy.

2. METHODS

Computational Details. The calculations were performed within plane wave basis set formulation of density functional theory (DFT) and the projector-augmented wave (PAW) method[32,33] as implemented in the Vienna ab initio simulation package (VASP).[34−37] The generalized gradient approximation (GGA) for the exchange correlation functional[38] and the plane wave cutoff of 450 eV were used. The valence configuration for the elements considered in this work is: $1s^1$ for H, $2p^6 3s^1$ for Na, $3p^6 4s^1$ for K, $2s^2 2p^3$ for N, $3s^2 3p^1$ for Al, $2s^2 2p^2$ for C, and $2s^2 2p^4$ for O.

The calculations of the solid phase were performed using k-point samplings such that in all cases the total energy is converged within 1 meV per formula unit. The Bader charge analysis[39−41] was performed using a Gaussian smearing with a width of 0.05 eV and the grid for the charge density with spacing of 0.04 Å or denser. The calculations of the densities of states were performed using the tetrahedron method.[42]

Analysis of the vibrational properties was done in the $2 \times 2 \times 1$ supercell and the harmonic approximation in the real space.[43,44] Dielectric properties and Born effective charges were calculated by the linear response method.[45] Additional details of calculations are given in the following sections.

Experimental Details. Ammonium, sodium, and potassium dawsonites, with chemical formulas $NH_4AlCO_3(OH)_2$, $NaAlCO_3(OH)_2$, and $KAlCO_3(OH)_2$, respectively, were prepared adapting the recipe of Fernández-Carrasco et al.[26] An appropriate amount of $Al(NO_3)_3 \cdot 9H_2O$ powder, corresponding to a concentration of 1 M, was added to aqueous solutions (2 M) of $(NH_4)_2CO_3$, Na_2CO_3, and K_2CO_3 at 353 K, yielding the corresponding dawsonites. The precipitation was carried out in a round-bottom glass vessel under reflux conditions and magnetic stirring (500 rpm). The resulting precipitate slurry was kept for 2 h at 353 K. The solids were filtered, washed with deionized water, and dried at 333 K for 12 h. In the manuscript, the nomenclature M-DW (M = Na^+, K^+, NH_4^+) makes reference to the as-synthesized materials as well.

Powder X-ray diffraction (XRD) was measured in a Siemens D5000 diffractometer with Bragg−Brentano geometry and Ni-filtered Cu Kα radiation (λ = 0.1541 nm). Data were recorded in the range 10−70° 2θ with an angular step size of 0.0168° and a counting time of 4 s per step.

Fourier transform infrared spectroscopy was carried out in a Bruker Optics Tensor 27 spectrometer equipped with a Golden Gate Diamond ATR unit. Spectra were collected at room temperature in the range 650−4000 cm^{-1} by coaddition of 32 scans at a nominal resolution of 4 cm^{-1}, taking the spectrum of the empty cell at ambient conditions as the background.

3. RESULTS AND DISCUSSION

3.1. Structural Properties. To ensure description of the crystalline ground state for the three dawsonites considered here, besides calculations for the known structures, we have performed a full search for the ground state structure by combination of structural optimization and simulated annealing method.[46,47] For the search of the ground state structures, the initial structures were constructed (i) from the structures of *Imma* and *Cmcm* symmetry where hydrogen atoms were added at a distance of 1 Å from oxygen at the 8i or 8g sites, and (ii) for $NH_4AlCO_3(OH)_2$ the ammonium groups were located at 4*c* lattice sites with four different initial orientations. Each initial structure for each compound was optimized with respect to the internal atomic positions with a conjugated gradient algorithm, followed by optimization of the unit cell shape and volume. Changes of the lattice angles below 1° were neglected. Next, all the structures were subjected to simulated annealing at constant volume, that is heating of the structures to 400 K over 1.5 ps with time step of 0.5 fs, and equilibration for 1.5 ps at T = 400 K. The applied time step is sufficient for the stability of the integration algorithm. During the equilibration process, the potential energy was monitored, and the structures at local energy minima were cooled to 10 K over 1.5 ps. Two structures for each compound with the lowest energy were optimized with a conjugated gradient algorithm with respect to the atomic positions and shape and volume of the unit cell. The symmetry analysis of these optimized structures provides an *Imma* space group for Na-DW and *Cmcm* for K-DW, as expected. For Na-DW, we follow the nomenclature of the International Tables for Crystallography.[24] The structures were reoptimized in constrained symmetry until the forces exerted on

dx.doi.org/10.1021/ic102443h |*Inorg. Chem.* 2011, 50, 2590–2598

Table 1. Internal Atomic Positions for Na-Dawsonite in *Imma* symmetry[a]

atom	Wyckoff site	*x/a*	*y/b*	*z/c*
Al	4b	0	0	0.5
Na	4c	0.25	0.25	0.25
C	4e	0	0.75	0.249
O	4b	0	0.75	0.127
O	8h	0	0.952	0.313
O	8i	0.180	0.75	0.525
H	8i	0.299	0.75	0.467

[a] Calculated lattice parameters are a = 6.862 (6.709) Å, b = 5.643 (5.599) Å, c = 10.393 (10.494) Å. The lattice constants determined from XRD measurements are shown in parentheses.

Table 2. Internal Atomic Positions for K-Dawsonite in *Cmcm* Symmetry[a]

atom	Wyckoff site	*x/a*	*y/b*	*z/c*
Al	4a	0.0	0.0	0.5
K	4c	0.0	0.346	0.25
C	4c	0.0	0.215	0.75
O	4c	0.0	0.323	0.75
O	8f	0.0	0.161	0.552
O	8g	0.193	0.986	0.75
H	8g	0.718	0.919	0.75

[a] Calculated lattice parameters are a = 6.547 (6.619) Å, b = 11.886 (11.631) Å, c = 5.728 (5.722) Å. The lattice constants determined from XRD measurements are shown in parentheses.

Table 3. Internal Atomic Positions for NH_4-Dawsonite in *Pnma* Symmetry[a]

atom	Wyckoff site	*x/a*	*y/b*	*z/c*
Al	4c	0.488	0.25	0.249
N	4c	0.765	0.75	0.111
C	4c	0.744	0.25	0.037
O	8d	0.238	0.064	0.233
O	4c	0.752	0.25	0.928
O	4c	0.543	0.25	0.088
O	4c	0.935	0.25	0.094
H	4c	0.658	0.75	0.041
H	4c	0.939	0.75	0.087
H	8d	0.736	0.874	0.162
H	8d	0.240	0.980	0.165

[a] Calculated lattice parameters are a = 5.785 (5.732) Å, b = 6.788 (6.607) Å, c = 11.849 (11.591) Å. The lattice constants determined from XRD measurements are shown in parentheses.

atoms were lower than 0.001 eV/Å. At the last step, the internal atomic positions were relaxed without symmetry that resulted in no further structural changes. Additional calculations were performed for NH_4-dawsonite constrained in *Cmcm* symmetry, as is discussed below.

The calculated structural properties for all three compounds considered in the present paper are shown in Tables 1′−3, and the structures are depicted in Figure 1. One has to note that the orientation of the unit cells with respect to Al−O layers is different for three dawsonites (Figure 1 and Tables 1′−3). In all

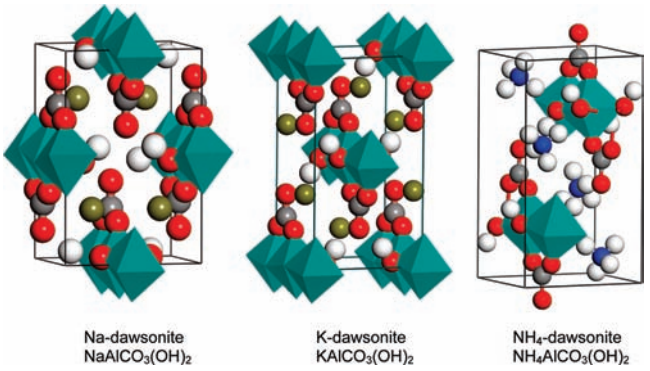

Figure 1. Structure of the unit cells of Na-, K-, and NH_4-dawsonite. Al: light blue octahedrons. C: gray spheres. O: red spheres. H: white spheres. Na and K: dark yellow spheres. N: dark blue spheres. Lattices are arranged for comparison of the layered structure of Al chains. Vertical axes are for *c*, *b*, *c* crystallographic axes, and horizontal axes are for *b*, *c*, *a*, respectively. The octahedrons show alignment of the Al−O chains in the structures.

the structures, the Al atoms are connected via oxygen anions, being arranged in the crystalline sheets parallel to the basal plane of the unit cell. Finally, these sheets are connected by OH^- groups and CO_3^{2-} ions. The arrangement of the atoms, as shown in Figure 1, indicates similarities between the structures (arrangement of AlO chains) and differences between $NaAlCO_3(OH)_2$ and the K- and NH_4-analogues considered here. The difference resides primarily in the arrangement of the cations (Na^+, K^+, NH_4^+) that are aligned in chains perpendicular to AlO sheets for Na-dawsonite and interchanged with CO_3^{2-} groups in the case of K-DW and NH_4-DW. Such a difference can be explained by the much smaller ionic radius for Na^+ (0.99 Å) as compared to that of K^+ (1.37 Å) or NH_4^+ (1.43 Å).[48] Differences in the cationic arrangement are accompanied by small differences in the local structure of the carbonate groups. In all the compounds, the CO_3^{2-} is distorted from the ideal D_{3h} symmetry, and the C−O bond lengths are 1.315 Å (2×) and 1.271 Å, respectively, in Na-DW. In K-DW these bonds are shorter, i.e., 1.307 Å and 1.286 Å, while in NH_4-DW, the carbonate group is strongly distorted with bonds of 1.283 1.299, and 1.312 Å, respectively, as a result of the strong interaction with the ammonium groups. One might note that Na-dawsonite in the *Cmcm* symmetry of the K-counterpart has the ground state electronic energy larger by 22.5 kJ/mol than that in *Imma*; for K-dawsonite, such a structural swap results in an energy increase by 26 kJ/mol.

The XRD diffraction patterns measured for the synthesized dawsonites are compared with the theoretical ones in Figure 2. For all dawsonites, there is a good agreement between previous experimental reports[23,25−27] and our XRD measurements. The error range for the lattice parameters is below 2%. For Na-dawsonite, the diffractogram is that determined for the calculated lattice parameters and displays small shifts of the reflections. Because the position of the diffraction peaks depends on the lattice parameters, which differ by 1−2% between experiment and calculations, for K- and NH_4-dawsonites, we have calculated the diffraction patterns for the theoretical structures where the lattice constants are adjusted to the experimental ones. This procedure provides proper location of the diffraction peaks and does not affect the diffraction pattern by any other means.

dx.doi.org/10.1021/ic102443h |*Inorg. Chem.* 2011, 50, 2590–2598

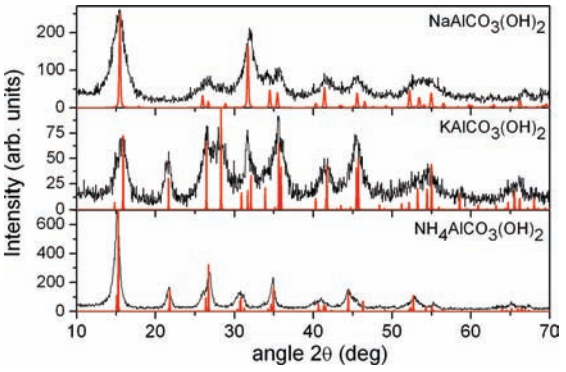

Figure 2. Calculated (red thick lines) and measured XRD patterns of Na-, K-, and NH_4-dawsonites.

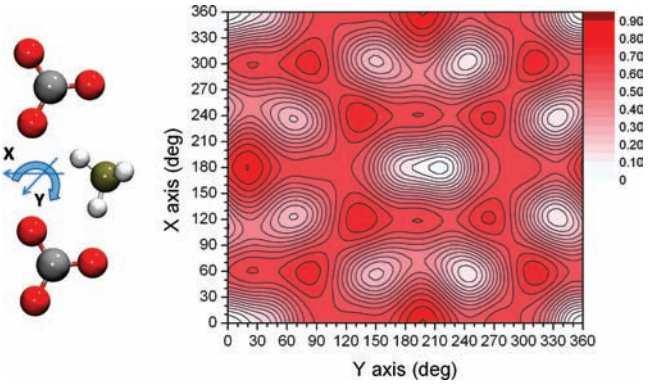

Figure 3. Potential energy surface for the NH_4^+ group in $NH_4AlCO_3(OH)_2$ with respect to rotation; energy scale is given in eV. Rotation axes are shown schematically in the left panel, where Y stands for rotation around axis parallel to *b*, and X is rotation around *a*. Multiple minima represent various equivalent orientations for NH_4^+; however, minima at (75, 120), (75, 240), (150, 60), and (150, 300) are local minima with different orientation. Local and global minima are separated by barriers of 0.3 eV or higher. The orientation of (30,0) is for the compound in *Cmcm* symmetry.

The structure of $NH_4AlCO_3(OH)_2$ reported by Iga and Kato[27] displays the base-centered *Cmcm* symmetry, the same as the K-analogue. This structure refinement, however, does not provide positions of the hydrogen atoms, neither these belonging to OH^- groups nor those of NH_4^+. We have determined the crystalline structure of $NH_4AlCO_3(OH)_2$ constrained in *Cmcm* symmetry, and it is shown that the positions of the heavy atoms are in good agreement with the data reported by Iga and Kato,[27] while the equilibrium positions of hydrogen are constrained by symmetry as indicated by the values in Table S1 of the Supporting Information. In this symmetry, the NH_4^+ groups are aligned along the *b* crystallographic axis with three edges of the tetrahedron in the *a*,*c* plane. Such a structure is however unstable and exhibits four imaginary modes (~ -250 cm^{-1}) at the center of the Brillouin zone (i.e., Γ point), thus indicating that the location of hydrogen in the lattice is important for NH_4-dawsonite. The ammonium group is a nonspherical cation that adopts its orientation in accordance to the lattice environment. The ordering of the NH_4^+ sublattice might influence the properties of NH_4-dawsonite at elevated temperatures, and a possible disorder is hardly observed in XRD experiments.

The computational search for the lowest energy-stable structure indicates that NH_4^+ groups are rotated along the *a* axis, which breaks the mirror site symmetry for the hydrogens located at the 8f and 8g sites in the *Cmcm* structure. Consequently, the primitive cell is doubled. The symmetry analysis of the lowest energy structures provides energetically equivalent structures that can be assigned to the $Cmc2_1$, $Pca2_1$, *Pm*, or *Pnma* space groups. Analysis of the normal modes indicates that a structure with *Pnma* symmetry does not have imaginary modes at the Γ point, and it is marginally (by 0.1 kJ/mol) more stable than other candidates. The ground state energy for *Pnma* symmetry is lower by 3 kJ/mol than that of *Cmcm* symmetry. The atomic positions and the lattice parameters are presented in Table 3. When the positions of hydrogen are not taken into account in the *Pnma* symmetry, the structure can be described as *Cmcm*, similarly as in Table S1 of the Supporting Information.

Because the calculations are performed for a static structure at 0 K, it is necessary to check the origin of the structural discrepancy between the calculated ground state structure and that experimentally determined by XRD for NH_4-dawsonite. As the symmetry difference originates primarily from the orientation of the ammonium cations, i.e., positions of hydrogen atoms that are hardly seen by X-ray diffraction experiments, we have analyzed a possible disorder in the ammonium ion sublattice in NH_4-dawsonite. For this purpose, we have determined the local potential energy surface as obeserved from the perspective of the NH_4^+ cationic group, which is subjected to independent rotation in the crystal. We have chosen rotation around the *a* and *b* lattice vectors of the *Pnma* structure. The potential energy surface is presented in Figure 3. The multiple minima at (0,0), (220,180), (340,120), (340,240), (250,60), and (250,300) correspond to the equivalent orientation of NH_4^+, while the local potential minima at (75,120), (75, 240), (150,60), and (150,300) correspond to distinct local energy minima with NH_4^+ orientation different than in the ground state. The energy barriers between minima are on the order of 0.3 eV, which suggest a possible disorder in the NH_4^+ sublattice above room temperature. However, the *Pnma* symmetry might be stable only at low temperatures.

3.2. Electronic Properties. The electronic structures of dawsonites are very similar, as presented in Figure 4. The three compounds display a wide band gap of E_g = 5.3 eV for Na-DW, E_g = 5.4 eV for K-DW, and E_g = 5.5 eV for NH_4-DW. The overall structure of the valence band is also similar with only a slightly larger orbital overlap for the K- and NH_4-dawsonites. The partial densities of states presented in Figure 4 indicate that the top of the valence band consists of oxygen orbitals, while the bottom of the conduction band is formed mostly by empty orbitals of carbon. The position of the empty states of cations differs between dawsonites. In Na-DW, the empty Na 4s state is localized ~9 eV above the top of the valence band, while for the other dawsonites, the empty states of cations are dispersed over a broad energy range of the conduction band. In the energy range from −5 eV to the Fermi level (which is defined at the top of the valence band) small perturbations present for K- and NH_4-DW suggest orbital overlap in this energy range that is not observed for Na-DW.

The calculated electronic structure provides insight into the atomic bonding via analysis of the charge distribution. The charge distribution calculated with the Bader method is presented in Table 4, where similarities and differences between the compounds can be identified. While the ionic charges on Al and hydrogen atoms belonging to hydroxyl groups are very similar for the three dawsonite structures, the charges on cations and

dx.doi.org/10.1021/ic102443h |*Inorg. Chem.* 2011, 50, 2590–2598

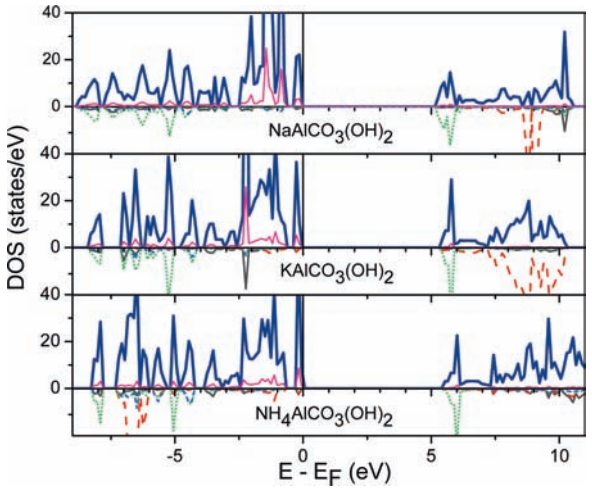

Figure 4. Electronic density of states (DOS) of dawsonites. Total DOS is shown with a thick blue line and partial DOS for oxygen with a thin fuchsia line. Partial density of states for Al (gray line), cation (Na, K, or N; dashed red line), C (dotted green line), and H (dashed blue line) are rendered below the total DOS with the axis inverted for clarity. Vertical scale for partial density of states is half of the scale for total DOS.

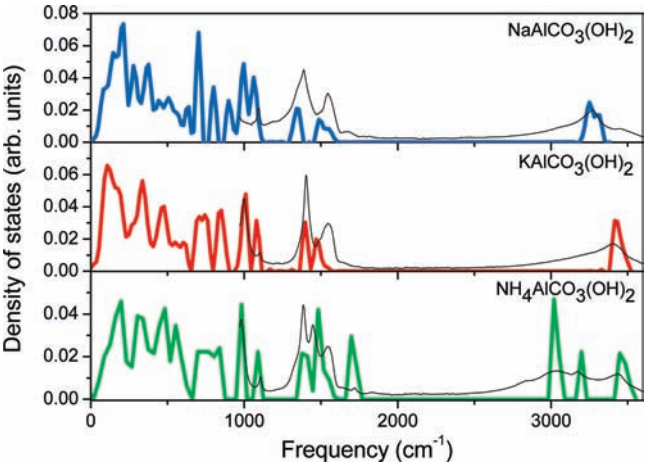

Figure 5. Phonon density of states of dawsonites. The band around 3400 cm^{-1} corresponds to OH local vibrations; bands around 1500 cm^{-1} are related to the local vibrations of CO_3^{2-}. For NH_4-dawsonite, additional bands around 3000 cm^{-1} and 1700 cm^{-1} are associated with local vibrations of NH_4^+ groups. Thin black lines represent experimental IR measurements, and they are shown for qualitative comparison of the positions of the peaks. Only spectra for modes above 1000 cm^{-1} are presented.

Table 4. Ionic Charges of Species Calculated for Dawsonites

species	Na-dawsonite	K-dawsonite	NH_4-dawsonite
Al	+2.48	+2.49	+2.49
cation	+0.88	+0.87	+0.79
CO_3	−1.70	−1.69	−1.66
O	−1.47	−1.46	−1.44
H	+0.65	+0.63	+0.63

carbonate groups differ. The charge on Na^+ and K^+ is ∼+0.9 e, very close to the formal charge of +1 e, while the ionic charge for the NH_4^+ group does not exceed +0.8 e. Additionally, the charge of the carbonate group is similar for the Na- and K-dawsonites, and it is lower for the NH_4-analogue as indicated in Table 4. Such a charge distribution suggests that all the compounds are strongly ionic. However, the lower ionic charges on the NH_4-DW may suggest a lower stability for this compound if other forms of interatomic interactions are not present. In fact, the charge distribution shown here shall be considered together with orbital hybridization (Figure 4), with the latter indicating covalent features of the bonds.

3.3. Vibrational Properties. The calculated ground state structures provide the starting point for vibrational analysis of dawsonites, which was done by displacements by ±0.02 Å of the symmetry independent atoms in the real space. The dynamical matrix was constructed from forces calculated for each displacement. Further details of the method can be found elsewhere.[43,44] However, it has to be noted that for large band gap insulators, as it is the case for the dawsonites considered herein, the nonanalytical part of the dynamical matrix in principle should be carefully considered because of the long-range Coulomb interactions, i.e., splitting of the infrared longitudinal and transverse modes. Thus, the Born effective charges and dielectric tensor were calculated by the linear response method for $NaAlCO_3(OH)_2$, as presented in the Table S2 of the Supporting Information. While the diagonal elements of the Born effective charge tensor are close to the Na^+ formal charge, for all the other elements, large deviations along diagonal and off-diagonal elements are observed. This is related to the directional covalent-like bonds in the carbonate ion and in the Al−OH chains. For simplicity reasons, we present data only for the transverse IR modes, which are directly available in the IR measurements. Such simplification does not affect the thermodynamic considerations presented below by more than 1 kJ/mol.

The calculated phonon density of states is shown in Figure 5. Good qualitative agreement between calculated density of states and measured by IR spectroscopy is observed. The overall similarity between the phonon spectra for the three structures originates from analogous distribution of the internal and lattice vibrations. The highest frequency bands localized above 3200 cm^{-1} are related to internal vibrations of the hydroxyl groups in the systems. Excitations localized around 1500 cm^{-1} are related to the internal vibrations of the carbonate groups, and those below 800 cm^{-1} are related to lattice vibrations. Coupling between these three groups provide additional features of the spectrum. However, there are significant differences between the three compounds. The systematic shift of the OH stretching modes around 3200 cm^{-1} can be seen for K- and NH_4-dawsonites with respect to Na-dawsonite (Figure 5) similar to the behavior observed experimentally by Serna et al.[28] In fact, the arrangement of O−H−C can be considered as a hydrogen bond of moderate strength.[49] The O−H−C bond lengths are 0.986 and 1.828 Å for K-dawsonite, 0.985 and 1.921 Å for NH_4-DW, and 0.995 and 1.707 Å for Na-DW, respectively. Shrinking of the O−H separation is in accordance with hardening of the O−H vibration. A larger separation between carbon and hydrogen in K- and NH_4-dawsonites suggest more electrostatic interactions within these bonds. In NH_4-dawsonite, the modes around 3000 cm^{-1} are related to the internal vibrations of the NH_4^+ groups.

In the region of the carbonate group internal vibrations, broad features are related to the degeneracy lifting for the symmetric bending (ν_4) and the asymmetric stretching (ν_3) modes. In $NH_4AlCO_3(OH)_2$, additional vibrations related to NH_4^+

Table 5. Normal Modes for Lattice Vibrations (cm^{-1})

	vibration mode[a]							
sample	*Au*	*Ag*	*B1g*	*B2g*	*B3g*	*B1u*	*B2u*	*B3u*
Na-dawsonite	141, 187, 319, 529, 1053	249, 354, 570, 697, 984, 1061, 1483, 3288	215, 370, 963	138, 204, 381, 434, 807, 915, 3228	150, 279, 499, 709, 1082, 1330	0, 162, 238, 379, 455, 492, 657, 699, 970, 1065, 1505, 3287	0, 142, 186, 290, 328, 524, 715, 984, 1359	0, 89, 201, 231, 266, 350, 661, 806, 907, 3240
K-dawsonite	129, 309, 495, 999	128, 266, 345, 552, 699, 856, 1068, 1442, 3456	79, 119, 176, 316, 427, 751, 821, 3418	192, 332, 987	101, 194, 296, 487, 721, 1018, 1395	0, 138, 196, 288, 361, 480, 727, 1002, 1385	0, 141, 382, 445, 495, 619, 709, 863, 1073, 1470, 3456	0, 103, 182, 242, 314, 612, 765, 823, 3426
NH_4-dawsonite	102, 134, 166, 204, 301, 315, 402, 465, 538, 565, 758, 822, 983, 1467, 1712	70, 149, 185, 235, 279, 295, 371, 391, 456, 476, 541, 697, 742, 821, 989, 1075, 1383, 1403, 1473, 1534, 1710, 3005, 3036, 3181, 3488	53, 139, 189, 199, 281, 310, 325, 506, 547, 617, 778, 818, (2) 977, 1474, 1713, 3023, 3461	115, 131, 196, 256, 297, 378, 451, 468, 486, 553, 601, 700, 730, 829, 995, 1086, 1382, 1403, 1494, 1520, 1725, 3014, 3058, 3184, 3505	93, 154, 158, 208, 303, 318, 404, 465, 529, 564, 778, 815, 984, 1474, 1716, (2)3013, (2) 3455	0, 140, 200, 254, 296, 393, 447, 457, 486, 507, 601, 706, 728, 851, 994, 1081, 1376, 1402, 1499, 1509, 1729, 3019, 3035, 3185, 3488	0, 150, 176, 197, 279, 310, 327, 502, 545, 611, 786, 817, 1465, 1710, 3022, 3462	0, 174, 193, 238, 292, 317, 383, 389, 455, 473, 538, 699, 740, 859, 988, 1079, 1380, 1414, 1494, 1589, 1723, 3016, 3042, 3197, 3520

[a] *B1u*, *B2u*, and *B3u* are infrared active modes, and *Ag*, *B1g*, *B2g*, and *B3g* are Raman active. Different orientations of the unit cells give the following relations between symmetry of the irreducible representations: $NaAlCO_3(OH)_2$ vs $KAlCO_3(OH)_2$ *B1u* ↔ *B2u* and *B1g* ↔ *B2g*, and $NaAlCO_3(OH)_2$ vs $NH_4AlCO_3(OH)_2$ *B2u* ↔ *B3u* and *B2g* ↔ *B3g* for infrared and Raman active modes, respectively. For $NH_4AlCO_3(OH)_2$, the number of modes corresponds to the calculated stable *Pnma* symmetry.

dx.doi.org/10.1021/ic102443h |*Inorg. Chem.* 2011, 50, 2590–2598

Table 6. Elastic Constants, Bulk and Young Modulus, and Poisson Ratio for Dawsonites[a]

	c_{11}	c_{12}	c_{13}	c_{23}	c_{22}	c_{33}	c_{44}	c_{55}	c_{66}	B_R	B_V	G_R	G_V	E	ν
Na-dawsonite	73	17	47	25	180	96	29	21	11	54	58	21	31	68	0.3
K-dawsonite	45	41	12	23	86	162	26	6	10	39	49	12	23	46	0.33
NH_4-dawsonite	157	19	31	28	45	77	12	29	9	38	48	16	23	51	0.3

[a] Values are given in GPa. Because of different orientations of the lattices in Na-, K-, and NH_4-dawsonites, there is the following interchange relation between constants: Na- and K-dawsonite, $c_{12} \leftrightarrow c_{13}$, $c_{22} \leftrightarrow c_{33}$, $c_{55} \leftrightarrow c_{66}$ and Na- and NH_4-dawsonite, $c_{11} \leftrightarrow c_{22}$, $c_{13} \leftrightarrow c_{23}$, $c_{44} \leftrightarrow c_{55}$.

are present in the frequency range of 1500−1700 cm^{-1}. The character of the lattice modes is similar for the samples containing NH_4^+ and K^+, a slightly different form of Na-dawsonite. This observation might be attributed also to the different mass of the metal cation.

The frequencies of all modes belonging to the irreducible representations for each compound are presented in Table 5. For the centered systems, there are 60 of such modes, and for NH_4-dawsonite in *Pnma* symmetry, there are 120 modes. For infrared active modes, we report only transverse mode frequencies. Partial assignment of the normal-mode frequencies for dawsonites was previously reported by Serna et al.[28] For Na- and K-dawsonites, there is excellent agreement between our calculations and previously reported data,[28] providing mode assignment for the Raman studies of various Na-DW.[50] However, in the present manuscript, we provide assignments for all the modes. It has to be mentioned that the peak in the frequency range of 3450 cm^{-1} does not belong to intrinsic modes of Na-DW, but it is related to the hydroxyl group stretching due to contamination, and thus it could serve as the indicator of compound purity.

In NH_4-dawsonite, the ammonium group is distorted from the ideal T_d symmetry. One of the N−H bonds is 1.037 Å, which is significantly shorter than 1.047 Å, and 1.046 Å for the remaining ones. The shortest bond is directed toward CO_3^{2-}. This distortion gives splitting of the high frequency internal vibrations of NH_4^+ located around 3000 and 3150 cm^{-1}. These features are present in the IR spectra.[28] Additionally, a distortion of NH_4^+ results in a variety of the active vibrations around 1725 and 1710 cm^{-1}. In this particular compound, the direct interaction of NH_4^+ with CO_3^{2-} gives rise to mode coupling/splitting for IR active modes around 1400 cm^{-1}. The modes *B*1*u* at 1505 cm^{-1} and *B*2*u* at 1359 cm^{-1} for Na-dawsonite [1470 and 1385 cm^{-1} for $KAlCO_3(OH)_2$] are multiplied in $NH_4AlCO_3(OH)_2$ as shown in Table 5; once the ammonium cations are disordered, some of these modes are not present.

The data presented in Table 5 can be useful as a guideline for proper mode assignment in vibrational spectroscopy studies that is sometimes difficult for experiments.

3.4. Elastic Properties. We have calculated all of the eight independent elastic constants (by applying strains on the unit cell) corresponding to the three dawsonites considered herein. The results are presented in Table 6. All the elastic constants are relatively small, and the largest constant ≤180 GPa is related to the compression−elongation along the Al−O chains. On the contrary, all the structures are softer with respect to the shear deformation related to the glide between Al−O chains. For all dawsonites, the elastic tensors possess positive eigenvalues that indicate stability of the structures.[51] Additionally, the shear is positive fulfilling Born criteria for crystal stability.[52] However, small numerical values for pure shear components (c_{66}) may suggest a low melting temperature that is related to the elastic properties of these crystals. The Cauchy relations $c_{44}/c_{23} = c_{55}/c_{13} = c_{66}/c_{12} = 1$ are generally not fulfilled in dawsonites (except for c_{44}/c_{23} in K-DW and c_{55}/c_{13} for NH_4-DW that are close to unity), but this criteria is valid only for structures that can be described by central forces acting between points of the lattice.[53] Dawsonites are layered molecular structures.

Additional characterization of the elastic properties is given by the bulk modulus, the Young modulus, and the Poisson ratio. These quantities were calculated as the approximation for the polycrystalline crystals following the Voigt (upper limit) and Reuss (lower limit) models.[53] Additionally, the bulk modulus for single crystals was calculated by uniform deformation of the unit cell and fitting of the total energy to the Murnaghan equation of state. The Voigt bulk and shear modulus[53] are $B_V = (c_{11} + c_{22} + c_{33})/9 + 2(c_{12} + c_{13} + c_{23})/9$, and $G_V = (c_{11} + c_{22} + c_{33} - c_{12} - c_{13} - c_{23})/15 + (c_{44} + c_{55} + c_{66})/5$, respectively, where c_{ij} are elastic constants. The Reuss values[53] are $B_R = [(s_{11} + s_{22} + s_{33}) + 2(s_{12} + s_{13} + s_{23})]^{-1}$, and $G_R = 15[4(s_{11} + s_{22} + s_{33}) - 4(s_{12} + s_{13} + s_{23}) + 3(s_{44} + s_{55} + s_{66})]^{-1}$, where s_{ij} are elastic compliances.[51] Formulas for the Young modulus (E) and Poisson ratio (ν) are given in the Supporting Information. The bulk, shear, and Young modulus presented in Table 6 are the largest for Na-DW, while the structural similarity between K-DW and NH_4-DW is reflected in similar values for *B*, *G*, and *E*. The bulk modulus for single crystalline dawsonites is B = 56.9 GPa, B = 47.6 GPa, and B = 47.8 GPa for Na-DW, K-DW, and NH_4-DW, respectively, that is in good agreement with the upper limit defined by B_V (Table 6). The low value of the Poisson ratio indicates that deviations from the central force solid are to be expected in dawsonites.

For anisotropic structures like dawsonites, it is instructive to examine anisotropy of the bulk and Young modulus, which are presented in Figures S1 and S2 of the Supporting Information. The bulk modulus for K-DW is significantly more anisotropic than for the other two dawsonites, while the anisotropy of shear modulus is similar for all the compounds. However, detailed analysis of the elastic properties is beyond the scope of the present paper.

3.5. Formation Energy. The enthalpy of formation is one of the fundamental properties of chemical compounds. It is calculated for dawsonites in the harmonic approximation on the basis of normal-mode analysis according to their decomposition into elements: $MAlCO_3(OH)_2 \rightarrow M + Al + C + 2.5O_2 + H_2$, where M = Na, K, or N (for NH_4-dawsonite, two additional H_2 molecules are considered). In the calculation, the formation enthalpy can be divided into static electronic (ΔE_0) and entropic (ΔU) contributions to the internal energy. The internal energy is defined as $\Delta U(T) = \Delta E_0 + \Delta U_0 + \Delta U_{ph}(T)$, where ΔU_0 corresponds to the zero point vibrations ($\Sigma_i \hbar\omega_i/2$), and $\Delta U_{ph}(T)$ is the energy related to the phonon distribution, i.e., $\Sigma_i \hbar\omega_i(\exp(\hbar\omega_i/kT) - 1)^{-1}$. The enthalpy equals $\Delta H(T) = \Delta U(T) + pV$. For solid phases, we assume the pressure−volume dependence to be negligible, while for the gas phases, we assume the $pV = kT$. The latter equation accounts for vibrational ($\Sigma_i \hbar\omega_i(\exp(\hbar\omega_i/kT) - 1)^{-1}$), rotational ($kT$), and translational

dx.doi.org/10.1021/ic102443h |*Inorg. Chem.* 2011, 50, 2590–2598

Table 7. Formation Enthalpy for Dawsonites[a]

compound	ΔE_0 (kJ/mol)	ΔH_0 (kJ/mol)	ΔH_{298} (kJ/mol)
K-dawsonite	−1816	−1753	−1714
Na-dawsonite	−1804	−1739	−1699
NH_4-dawsonite	−1820	−1686	−1655

[a] ΔE_0 is the electronic contribution to the binding energy, ΔH_0 is the formation enthalpy at $T = 0$ K, and ΔH_{298} is the formation enthalpy at $T = 298$ K.

$(3kT/2)$ degrees of freedom, respectively. Thus, three quantities, i.e., ΔE_0, $\Delta H_0 = \Delta E_0 + \Delta U_0$, and $\Delta H_{298} = \Delta H_0 + \Delta U_{ph}(298)$ (enthalpy of formation at 298 K) are defined as presented in Table 7. The electronic contribution, ΔE_0 (that origins form ionic, covalent, and other forms of static bonding), to the formation energy is the largest for NH_4-dawsonite and the smallest for Na-dawsonite as shown in Table 7. This result indicates that in $NH_4AlCO_3(OH)_2$, besides the ionic interaction, covalent features of the bonding are important. The vibrational entropy lowers the stability such that at standard thermodynamic conditions $KAlCO_3(OH)_2$ is the most stable, followed by $NaAlCO_3(OH)_2$ and $NH_4AlCO_3(OH)_2$. The calculated formation enthalpy for Na-dawsonite (−1699 kJ/mol) is in good agreement with that reported by calorimetry methods by Bénézeth et al. (−1782 kJ/mol).[54] The underestimation by ∼5% can be attributed to approximations for the exchange−correlation functional and harmonic approximations for the finite temperature properties applied here. The ordering of the formation enthalpy ΔH_{298} presented in Table 7 is in agreement with the thermal stability of dawsonites determined by thermogravimetry.[20] K-dawsonite is slightly more stable than Na-dawsonite, while the stability of NH_4-dawsonite is lower.

4. CONCLUSIONS

This manuscript reports for the first time a systematic DFT and thus far most comprehensive study on the structural and essential physicochemical properties, i.e., vibrational, electronic, elastic, and formation energy, of three dawsonite compositions, namely, $NaAlCO_3(OH)_2$, $KAlCO_3(OH)_2$, and $NH_4AlCO_3(OH)_2$. The computational results are in excellent agreement with the experimental data. Our results confirm the *Imma* and *Cmcm* structures for Na- and K-dawsonites, while for NH_4-dawsonite, we propose the *Pnma* symmetry, which is dynamically stable unlike the previously reported *Cmcm* configuration. However, the calculations indicate the possibility of NH_4 disorder at elevated temperatures. The calculated formation enthalpy provides the following stability order, K-dawsonite > Na-dawsonite > NH_4-dawsonite, that is matching previous thermal analysis and aqueous solution stability empirical observations. We show that three dawsonites are strongly ionic systems. The comparison of the three analogues provides comprehensive insight into diversity of dawsonite intrinsic properties, and such insight is required for future tuning of their applications, with particular focus on the CO_2 capture applications. As the realistic process of CO_2 trapping and storage by dawsonites is rather complex, our study provides a first step toward detailed understanding of dawsonites.

■ ASSOCIATED CONTENT

Supporting Information. Crystal structures of NH_4-dawsonite in *Cmcm* symmetry, Born effective charges and dielectric tensor for $NaAlCO_3(OH)_2$, and schematic illustrations of bulk modulus and Young modulus. This material is available free of charge via the Internet at http://pubs.acs.org.

■ AUTHOR INFORMATION

Corresponding Author

* E-mail: Zbigniew.Lodziana@ifj.edu.pl.

■ ACKNOWLEDGMENT

Z.Ł. kindly acknowledges support by MNiSW Project N N202 207138 and CPU allocation at ACK Cyfronet, Kraków. G.S. and J.P.R. kindly acknowledge ETH support. This manuscript was improved by thorough and constructive suggestions of anonymous reviewers.

■ REFERENCES

(1) Harrington, B. J. *Canadian Naturalist* **1874**, *7*, 305.
(2) Serna, C. J.; White, J. L.; Hem, S. L. *J. Pharm. Sci.* **1978**, *67*, 324.
(3) Ali, A. A.; Hasan, M. A.; Zaki, M. I. *Chem. Mater.* **2005**, *17*, 6797.
(4) Yalfani, M. S.; Santiago, M.; Pérez-Ramírez, J. *J. Mater. Chem.* **2007**, *17*, 1222.
(5) Stoica, G.; Santiago, M.; Jacobs, P. A.; Pérez-Ramírez, J.; Pescarmona, P. P. *Appl. Catal., A* **2009**, *371*, 43.
(6) Gaus, I. *Int. J. Greenhouse Gas Control* **2010**, *4*, 73.
(7) Hellevang, H.; Aagaard, P.; Oelkers, E. O.; Kvamme, B. *Environ. Sci. Technol.* **2005**, *39*, 8281.
(8) Baker, J. C.; Bai, G. P.; Hamilton, J.; Golding, S. D.; Keene, J. B. *J. Sediment. Res.* **1995**, *A65*, 522.
(9) Walspurger, S.; Cobden, P. D.; Haije, W .G.; Westerwaal, R.; Elzinga, G. D.; Safonova, O. V. *Eur. J. Inorg. Chem.* **2010**, *17*, 2461.
(10) Santiago, M.; Pérez-Ramírez, J. *Environ. Sci. Technol.* **2007**, *41*, 1704.
(11) Masuda, T.; Watanabe, T.; Miyahara, Y.; Kanai, H.; Inoue, M. *Top. Catal.* **2009**, *52*, 699.
(12) Stoica, G.; Abelló, S.; Pérez-Ramírez, J. *Appl. Catal. A* **2009**, *365*, 252.
(13) Gunter, W. D.; Perkins, E. H.; McCann, T. J. *Energy Convers. Manage.* **1993**, *34*, 941.
(14) Worden, R. H. *Mar. Pet. Geol.* **2006**, *23*, 67.
(15) Marini, L. *Developments in Geochemistry*; Elsevier: Amsterdam, 2007; Vol. 11, p 100.
(16) Ryzhenko, B. N. *Geochem. Int.* **2004**, *44*, 835.
(17) Kaszuba, J. P.; Janecky, D. R.; Snow, M. G. *Chem. Geol.* **2005**, *217*, 277.
(18) Zerai, B.; Saylor, B. Z.; Matisoff, G. *Appl. Geochem.* **2006**, *21*, 223.
(19) Hangx, S. J. T.; Spiers, C. J. *Chem. Geol.* **2009**, *265*, 88.
(20) Stoica, G.; Pérez-Ramírez, J. *Geochim. Cosmochim. Acta* **2010**, *74*, 7048.
(21) Stoica, G.; Groen, J. C.; Abelló, S.; Manchanda, R.; Pérez-Ramírez, J. *Chem. Mater.* **2008**, *20*, 3973.
(22) Lauro, C. *Rend. Accad. Ital.* **1941**, *3*, 146.
(23) Frueh, A. J.; Golightly, J. P. *Canadian Mineralogist* **1967**, *9*, 51.
(24) Hahn, T. *International Tables for Crystallography*, 5th ed.; Springer: Dordrecht, The Netherlands, 2005; Vol. A: Space-Group Symmetry.
(25) Corazza, E.; Sabelli, C.; Vannucci, S. *Neues Jahrb. Mineral., Monatsh.* **1977**, *9*, 381.
(26) Fernández-Carrasco, L.; Puertas, F.; Blanco-Varela, M. T.; Vázquez, T.; Rius, J. *Cem. Concr. Res.* **2005**, *35*, 641.
(27) Iga, T.; Kato, S. *J. Ceram. Soc. Jpn.* **1978**, *86*, 509.
(28) Serna, C. J.; Garcia-Ramos, J. V.; Peña, M. J. *Spectrochim. Acta* **1985**, *41A*, 697.

(29) Hernández, M. J.; Ulibarri, M. A.; Cornejo, J.; Peña, M. J.; Serna, C. J. *Thermochim. Acta* **1985**, *94*, 257.
(30) Nørskov, J. K.; Bligaard, T.; Rossmeisl, J.; Christensen, C. H. *Nature Chem.* **2009**, *1*, 37.
(31) Catlow, C. R. A.; Guo, Z. X.; Miskufova, M.; Shevlin, S. A.; Smith, A. G. H.; Sokol, A. A.; Walsh, A.; Wilson, D. J.; Woodley, S. M. *Philos. Trans. R. Soc., A* **2010**, *368*, 3379.
(32) Kresse, G.; Joubert, D. *Phys. Rev. B* **1999**, *59*, 1758.
(33) Blöchl, P. E. *Phys. Rev. B* **1994**, *50*, 17953.
(34) Kresse, G.; Furthmüller, J. *Phys. Rev. B* **1996**, *54*, 11169.
(35) Kresse, G.; Furthmüller, J. *Comput. Mater. Sci.* **1996**, *6*, 15.
(36) Kresse, G.; Hafner, J. *Phys. Rev. B* **1993**, *47*, 558.
(37) Hafner, J. *J. Comput. Chem.* **2008**, *29*, 2044.
(38) Perdew, J. P.; Burke, K.; Ernzerhof, M. *Phys. Rev. Lett.* **1996**, *77*, 3865.
(39) Bader, R. *Atoms in Molecules: A Quantum Theory*; Oxford University Press: New York, 1990.
(40) Henkelman, G.; Arnaldsson, A.; Jónsson, H. *Comput. Mater. Sci.* **2006**, *36*, 354.
(41) Sanville, E.; Kenny, S. D.; Smith, R.; Henkelman, G. *J. Comput. Chem.* **2007**, *28*, 899.
(42) Blöchl, P. E.; Jepsen, O.; Andersen, O. K. *Phys. Rev. B* **1994**, *49*, 16223.
(43) Łodziana, Z.; Parlinski, K. *Phys. Rev. B* **2003**, *67*, 174106.
(44) Baroni, S.; de Gironcoli, S.; Dal Corso, A.; Giannozzi, P. *Rev. Mod. Phys.* **2001**, *73*, 515.
(45) Gajdos, M.; Hummer, K.; Kresse, G.; Furthmüller, J.; Bechstedt, F. *Phys. Rev. B* **2006**, *73*, 045112.
(46) Woodeley, S. M.; Catlow, R. *Nat. Mater.* **2008**, *7*, 937.
(47) Łodziana, Z.; Vegge, T. *Phys. Rev. Lett.* **2004**, *93*, 145501.
(48) Shannon, R. D. *Acta Crystallogr., Sect. A: Cryst. Phys., Diffr., Theor. Gen. Crystallogr.* **1976**, *32*, 751.
(49) Steiner, T. *Angew. Chem., Int. Ed.* **2002**, *41*, 48.
(50) Sirbescu, M.-L. C.; Nabelek, P. I. *Am. Mineral.* **2003**, *88*, 1055.
(51) Nye, J. F. *Physical Properties of Crystals*; Oxford University Press: London, 1957.
(52) Born, M. *J. Chem. Phys.* **1939**, *7*, 591.
(53) Cowin, S. C. *J. Mech. Appl. Math.* **1989**, *42*, 249.
(54) Bénézeth, P.; Palmer, D. A.; Anovitz, L. M.; Horita, J. *Geochim. Cosmochim. Acta* **2007**, *71*, 4438.